Revision 5: 4/2/97

Mean-field analysis and Monte Carlo study of an interacting two-species catalytic surface reaction model

K. S. Brown, K. E. Bassler, D. A. Browne
Department of Physics and Astronomy, Louisiana State University, Baton Rouge, Louisiana 70803

(February 1, 2008)

Abstract

We study the phase diagram and critical behavior of an interacting one dimensional two species monomer-monomer catalytic surface reaction model with a reactive phase as well as two equivalent adsorbing phase where one of the species saturates the system. A mean field analysis including correlations up to triplets of sites fails to reproduce the phase diagram found by Monte Carlo simulations. The three phases coexist at a bicritical point whose critical behavior is described by the even branching annihilating random walk universality class. This work confirms the hypothesis that the conservation modulo 2 of the domain walls under the dynamics at the bicritical point is the essential feature in producing critical behavior different from directed percolation. The interfacial fluctuations show the same universal behavior seen at the bicritical point in a three-species model, supporting the conjecture that these fluctuations are a new universal characteristic of the model.

05.70.Ln, 82.20.Mj, 82.65.Jv, 64.60.Kw

I. INTRODUCTION

Nonequilibrium statistical models with many degrees of freedom whose dynamics violate detailed balance arise in many areas such as biological populations, chemical reactions, fluid turbulence, traffic flow, and growth/deposition processes. The macroscopic behavior of these models can be much richer than that of systems in thermal equilibrium, showing organized macroscopic spatial and temporal structures like pulses or waves, and even spatiotemporal chaos. Even the steady state behavior of a homogeneous system without these structures can be far more complicated, involving for example a scale invariant steady state without tuning the system to a specific point. However, like their equilibrium cousins, systems at continuous transitions between nonequilibrium steady states show universal behavior that is insensitive to microscopic details and depends only on properties such as symmetries and conservation laws.

One class of models that have received extensive study are those with absorbing phase transitions where the system changes from an active state with statistical fluctuations about the mean behavior to a noiseless inert state consisting of a single microscopic configuration. The term absorbing refers to the fact that the system cannot leave this state once it reaches it. Examples include directed percolation (DP) [1,2], the contact process [3], auto-catalytic reaction models [4], and branching annihilating random walks with odd numbers of offspring [5,6]. Both renormalization group calculations [1,7] and Monte Carlo simulations [2–6,8] show that these models form a single universality class for a purely nonequilibrium model with no internal symmetry in the order parameter.

Recently, a number of models with continuous adsorbing transitions in a universality class distinct from directed percolation have been studied. These models include probabilistic cellular automata models studied by Grassberger and coworkers [9], certain kinetic Ising models [10], the interacting monomer-dimer model [11], a three species monomer model with Potts-like symmetry [12,13] and branching annihilating random walks with an even number of offspring (BAWe) [5,14]. All of these models except for the BAWe have two equivalent absorbing states indicating the importance of symmetry of the adsorbing state to the universality class. However, the universal behavior of this new class is apparently controlled by a dynamical conservation law. If the important dynamical variables in this class are defects represented by the walkers in the BAWe model and the walls between different saturated domains in the other models, the models have a "defect parity" conservation law [9] where the number of defects is conserved modulo 2. Recent field theoretic work confirms this viewpoint [15].

Recently, two of us [12,13] investigated a three-species monomer model with annihilation reactions between dissimilar species. The transitions from the reactive state to a single absorbing state where one species saturates the system fell in the DP universality class. These phase boundaries meet at bicritical points [16] where two different absorbing states coexist. Because the domain walls between different domains of the two phases spawn and annihilate in pairs, the critical behavior fell into the BAWe universality class. We also showed that at the bicritical point the characteristic fluctuations of the domain walls between the equivalent absorbing phases was given by a new exponent.

The present paper studies the connection between the behavior at a bicritical point and the presence of the BAWe critical behavior and tests the universality of the interfacial

fluctuations. We investigate a model introduced by Zhuo, Redner, and Park [17] that also has a bicritical point at the junction of two absorbing phase transitions. We find that the bicritical exponents in this model also fall into the BAWe class and the interfacial exponents are the same as in the three species model, lending credence to the universal nature of the interfacial fluctuations.

In the next section we introduce the model and present results for the mean field theory in two levels of approximation. Section 3 discusses our static and dynamic Monte Carlo simulations that yield a different phase diagram from the mean field results and produce critical exponents for the dynamic behavior that fall into the BAWe class. The final section contains our conclusions.

II. THE MODEL

The model we study was first introduced by Zhuo, Park and Redner [17]. Two monomers, called A and B, adsorb at the vacant sites of a one-dimensional lattice with probabilities p and q, respectively, where $p + q = 1$. The adsorption of a monomer at a vacant site is affected by monomers present on neighboring sites. If either neighboring site is occupied by the same species as that trying to adsorb, the adsorption probability is reduced by a factor $r < 1$, mimicking the effect of a nearest-neighbor repulsive interaction. Unlike monomers on adjacent sites react immediately and leave the lattice, leading to a process limited only by adsorption. We have performed static Monte Carlo simulations that produce a phase diagram similar to the one found by Zhuo *et al.* [17]. The diagram, displayed in Fig. 1 with p plotted *vs.* r, shows a reactive steady state (R) bordered by two equivalent saturated phases (labeled A and B). The transitions from the reactive phase to either of the saturated phases are continuous, while the transition between the saturated phases is first-order discontinuous. The two saturated phases meet the reactive phase at a *bicritical* point [16] at a critical value of $r = r_c$. In the case of $r = 1$, the reactive region no longer exists [18,19] and the only transition line is the first-order discontinuous line between the saturated phases. Another model in which the adsorption repulsion is not symmetric (only A's feel the repulsion) has been studied [17], and its critical behavior was found to be in the DP universality class. However, no effort was made to determine either the location of the bicritical point or the bicritical behavior of the model.

III. MEAN-FIELD THEORY

To analyze the kinetics of this model, it is useful to perform a mean-field analysis. While such analysis neglects long-range correlations and thus cannot be expected to properly predict critical properties, it should properly predict the qualitative structure of the phase diagram, including the existence of continuous transitions and multi-critical points. The mean-field analysis also provides a starting point for studying the importance of such fluctuations, which become particularly important near continuous phase transitions. The mean-field approach we use [20] studies the time evolution of clusters of sites, the approximation coming in truncating the probabilities of observing clusters of larger size into probabilities

for smaller size clusters. The analysis presented below of this 1D model includes clusters consisting of up to triplets of adjacent sites.

At a particular time, a lattice with N sites will have N_V vacancies, the remaining sites being filled with N_A A monomers and N_B B monomers. The density of species $i = A$, B, V is $x_i \equiv (N_i/N)$. We have the obvious constraint

$$x_V + x_A + x_B = 1, \tag{1}$$

so we can take x_A and x_B as independent.

We next consider clusters of pairs of sites, where we define N_{ij} as the number of pairs with species i on one site and j on the site to its right, and the pair density $x_{ij} \equiv (N_{ij}/N)$. Because of the immediate reaction of AB pairs we have $N_{AB} = N_{BA} = 0$. Using relations between the pair and site occupancies

$$\begin{aligned} x_A &= x_{AA} + x_{AV} = x_{VA} + x_{AA} \\ x_B &= x_{BB} + x_{BV} = x_{VB} + x_{BB} \\ x_V &= x_{AV} + x_{BV} + x_{VV}, \end{aligned} \tag{2}$$

only two of the pair densities are independent of the x_i, which we choose to be x_{AA} and x_{BB}.

For the clusters of triples we define N_{ijk} as the number of triples with species j in the central site, species i to the left, and species k to the right, with the corresponding densities $x_{ijk} = (N_{ijk}/N)$. The prohibition of adjacent AB pairs and the relations between the numbers of clusters of triples and pairs of sites

$$\begin{aligned} x_{AA} &= x_{AAV} + x_{AAA} &&= x_{VAA} + x_{VVV} \\ x_{AV} &= x_{AVV} + x_{AVA} + x_{AVB} &&= x_{VAV} + x_{AAV} \\ x_{VA} &= x_{VVA} + x_{AVA} + x_{BVA} &&= x_{VAV} + x_{VAA} \\ x_{BB} &= x_{BBV} + x_{BBB} &&= x_{VBB} + x_{BBB} \\ x_{BV} &= x_{BVV} + x_{BVA} + x_{BVB} &&= x_{VBV} + x_{BBV} \\ x_{VB} &= x_{VVB} + x_{AVB} + x_{BVB} &&= x_{VBV} + x_{VBB} \\ x_{VV} &= x_{VVV} + x_{VVA} + x_{VVB} &&= x_{VVV} + x_{AVV} + x_{BVV} \end{aligned} \tag{3}$$

gives a total of 6 independent triple densities: x_{AAA}, x_{AVA}, x_{BBB}, x_{BVB}, x_{AVB}, and x_{BVA}. The last two are equal in a homogeneous steady state.

We must calculate the rate that each of these densities change due to four allowed kinetic processes: deposition of an A without reaction, removal of an A by reaction with a B adsorbing next to it, deposition of a B without reaction, and removal of a B by reaction by an adsorbing A. These four processes are detailed in Table I. Because of the symmetry of the reaction rules, we will usually only present explicit formulae for half of the equations; the remainder can be found by interchanging A and B everywhere in the equations.

The exact equations for the single site densities are

$$\begin{aligned} \frac{dx_A}{dt} = {} & p\, x_{VVV} + p\, r\, (x_{VVA} + x_{AVV} + x_{VAV}) \\ & - q\, (x_{VVA} + x_{AVV} + x_{VAV}) \\ & - q\, r\, (x_{AVB} + x_{BVA}) \end{aligned}$$

$$\begin{aligned}\frac{dx_B}{dt} &= q\,x_{VVV} + q\,r\,(x_{VVB} + x_{BVV} + x_{VBV}) \\ &\quad - p\,(x_{VVB} + x_{BVV} + x_{VBV}) \\ &\quad - p\,r\,(x_{BVA} + x_{AVB}) \end{aligned} \tag{4}$$

which clearly shows the $A \leftrightarrow B$ symmetry noted above.

By considering each of the possible reactions in Table I, the equation for the AA pairs is

$$\begin{aligned}\frac{dx_{AA}}{dt} &= p\,r\,(x_{VVA} + x_{AVV} + 2x_{AVA}) \\ &\quad - q\,(x_{VVAA} + x_{AAVV} + \frac{1}{2}x_{AAVA} + \frac{1}{2}x_{AVAA}) \\ &\quad - q\,r\,(x_{AAVB} + x_{BVAA}) \end{aligned} \tag{5}$$

where we have denoted densities of quartets of sites in an obvious extension of our notation.

Finally the triples obey the equations

$$\begin{aligned}\frac{dx_{AAA}}{dt} &= p\,r\,(x_{VVAA} + x_{AAVV} + x_{AVA} + x_{AVAA} + x_{AAVA}) \\ &\quad - q\,(x_{VVAAA} + x_{AAAVV} + \frac{1}{2}x_{AAAVA} + \frac{1}{2}x_{AVAAA}) \\ &\quad - q\,r\,(x_{AAAVB} + x_{BVAAA}) \\ \frac{dx_{AVA}}{dt} &= p\,(x_{VVVA} + x_{AVVV}) - p\,r\,x_{AVA} \\ &\quad - q\,(x_{VVAVA} + x_{AVAVV} + x_{AVAVA} + x_{AVA}) \\ &\quad - q\,r\,(x_{AVAVB} + x_{BVAVA}) \\ \frac{dx_{AVB}}{dt} &= p\,x_{VVVB} + q\,x_{AVVV} \\ &\quad - q\,(x_{VVAVB} + \frac{1}{2}x_{AVAVB}) - p\,(x_{AVBVV} + \frac{1}{2}x_{AVBVB}) \\ &\quad - q\,r\,(x_{AVB} + x_{BVAVB}) - p\,r\,(x_{AVB} + x_{AVBVA}) \end{aligned} \tag{6}$$

In general, for a cluster of M sites, the adsorption processes link clusters of M sites to clusters of $M+1$ sites and the reaction processes link to clusters of $M+2$ sites.

To close the equations we perform a truncation. In the site approximation, we ignore any spatial correlations and solve just Eqn. (4) — and its partner for x_B – using Eqn. (1) and the approximation $x_{ijk} \approx x_i x_j x_k$. We find the boundary between the saturated A phase and the reactive phase by finding the combination of parameters p and r where the saturated phase fixed point loses its stability. This occurs when $p = 1/(1+r)$. The B-saturated phase boundary is given by $q = 1 - p = 1/(1+r)$. These are shown as dashed lines in Fig. 2. The absorbing state transitions are continuous but there is no coexistence line between the saturated phases, just as we found in Ref. [13].

In the pair approximation, we replace correlations of triples and larger clusters of sites by approximating them as $x_{ijk} = x_{ij}(x_{jk}/x_j)$, and $x_{ijkl} = x_{ij}(x_{jk}/x_j)(x_{kl}/x_k)$. Each term in parentheses like (x_{jk}/x_j) has the simple interpretation as the conditional probability of finding species k given that the site to the left is occupied by species j. We again find the

phase diagram by determining where the stability of the poisoned phase fixed point of the system of Eqns. (4) and (5) vanishes. Unlike the site approximation, solving the equations to determine the phase boundary was determined numerically. This procedure required some care because, although terms like x_{VA} and x_V vanish on the phase boundary, their ratio, which appears in Eqns. (4) and (5) in our approximation, is nonzero. We note that, just as for the three species model [13], Fig. 2 shows that this approximation fails to produce the coexistence curve between the saturated phases. This indicates that the large domains of A and B that appear close to the absorbing phase transitions are not accurately represented in the site and pair approximations. In both of these approximations, the width of the reactive window is proportional to $(1-r)$ as r approaches one.

The triple approximation is similar in spirit to the pair approximation with higher order correlations being decomposed as conditional probabilities via $x_{ijkl} \approx x_{ijk}(x_{jkl}/x_{jk})$ and $x_{ijklm} \approx x_{ijk}(x_{jkl}/x_{jk})(x_{klm}/x_{kl})$. The numerically determined phase diagram is shown in Fig. 2 and shows little difference from the pair approximation except very close to $r = 1$. Surprisingly, the triple approximation fails here to move the bicritical point away from $r = 1$, which did happen in our earlier work [13] on the three-species model. Very close to $r = 1$, the width of the reactive region varies as $(1-r)^{3/2}$ in this approximation.

We stop the mean field approach at the triple approximation because the increase in algebra is not compensated by an improvement of the phase diagram. The failure of this mean field approach to produce a realistic position for the bicritical point is linked to the fact that the probability of observing a long cluster of sites all filled with one species, which is approximated here by the probability of a smaller cluster raised to a power, will decay exponentially with the size of the cluster. However, the simulations presented in this paper and previous work [12,13] clearly show that at the bicritical point large domains of each species are present in the steady state, with the fundamental dynamical variables being the domain walls.

IV. SIMULATIONS

The behavior of this model at the critical lines has been studied and found to be in the DP universality class [17], which we verified using 10^5 independent runs of up to 10^4 time steps. What has not been studied is the behavior at the bicritical point. We use two types of "epidemic" simulations [6,14,21] to study the system's behavior at the bicritical point. The first (defect dynamics) starts with the lattice in a configuration close to one of the saturated phases, in which a lone vacancy is surrounded by members of one species. The second (interface dynamics) studies the time evolution of a minimum-width interface between the two saturated phases (a lone vacancy is bordered on one side by A's and by B's on the other side). In the defect dynamics, the simulations are over when the lattice becomes totally saturated. For the interface dynamics the end of the simulation is marked by the "collapse" of the interface back to its minimum width [12].

Since the total number of possible adsorption sites is usually very small, we use a variable time algorithm to improve computational efficiency. A list of possible adsorption sites is kept during the simulation, and one of these sites is picked at random for adsorption according to $\{p_\alpha\}$ and, if applicable, r. Time is then incremented by $1/n_V(t)$, where $n_V(t)$ is the number

of vacancies in the lattice at that time. To avoid end effects, we always start with a lattice that is so large as to be considered of infinite extent.

During the defect dynamics simulations, we measure $P(t)$, the probability that the system will not become saturated at time t, $n_V(t)$, the number of vacancies in the lattice at time t, $n_o(t)$, the number of species opposite to those of the initial saturated configuration at time t, and $R^2(t)$, the square size of the reactive region in a surviving run at time t. At a continuous phase transition as $t \to \infty$ these quantities obey power laws

$$P(t) \propto t^{-\delta} \;\; \langle R^2(t) \rangle \propto t^{z} \;\; \langle n_V(t) \rangle \propto t^{\eta} \;\; \langle n_o(t) \rangle \propto t^{\eta_o} \tag{7}$$

The exponent η_o is not independent of the others, but gives a useful check on the calculation. The scaling law for η_o can be understood by considering the set of all surviving runs. The width of the defect region grows as $t^{z/2}$. This region is filled with vacants and sites occupied by either of the species, so $[R^2(t)]^{1/2} = c(n_V + n_A + n_B)P(t)$, with c some constant. The factor $P(t)$ accounts for the fact only the surviving runs contribute to $R^2(t)$. If we further assume that in this defect (which is very large for long times since $z > 0$) we have the same kind of configurations as we would see in a static simulation, we should have $n_o = N_A(t) = N_B(t)$. Thus we should see

$$2n_o(t) = \frac{[R^2(t)]^{1/2}}{cP(t)} - n_V(t) \sim c_1 t^{z/2-\delta} - c_2 t^{\eta} \tag{8}$$

so we see that $\eta_o = (z/2) - \delta$.

For the interface dynamics simulations, we define $P(t)$ to be the probability of the interface of avoiding collapse back to minimum width, with $n(t)$ the vacancy concentration and $R^2(t)$ the square-size of the interface, both similar to the above. $n_o(t)$ has no meaning or corresponding equivalent in this type of simulation, so it is not measured. As $t \to \infty$ these quantities obey power laws

$$P(t) \propto t^{-\delta'}, \quad \langle n(t) \rangle \propto t^{\eta'}, \quad \langle R^2(t) \rangle \propto t^{z'}. \tag{9}$$

Log-log plots of these measured quantities as a function of time are straight lines at a phase transition and show curvature away from transitions. A precise estimate for both the location of the bicritical point and the values of the exponents can be obtained by examining the local slopes of the curves on a log-log plot. For example, the effective exponent $-\delta(t)$ is defined as

$$-\delta(t) = \{\ln[P(t)/P(t/b)]/\ln b\}, \tag{10}$$

with similar definitions for $\eta(t)$, $\eta_o(t)$, and $z(t)$. We usually choose $b = 5$ for our numerical work, with other values like $b = 2$ and $b = 3$ being used to check the results. At the bicritical point, the value of the effective exponent should extrapolate to the bicritical value in the long time limit ($t^{-1} \to 0$). Away from the bicritical point, the local slope will show strong upward or downward curvature as $t^{-1} \to 0$.

To determine the value of both the critical exponents and their uncertainties, we use a technique different from that typically employed [6,22]. The data collected at the bicritical point is divided into ten data sets that are statistically independent. A linear regression is

then performed on each set, with the intercept the only pertinent quantity. The value for the exponent is then calculated as the simple mean of the ten intercepts, and the uncertainty is the standard error of the mean. All of the results quoted in this paper were obtained using this technique, which gives a more unbiased estimate of the uncertainty than previous methods which used the quality of the linear fit to the entire data set.

Figure 3 shows the local slopes of the data for the defect dynamics simulations for $p = 0.5$ and r near the bicritical value. The system started near an A saturated phase, but the symmetry of the model dictates that we could equally as well have started near a B saturated phase. This data was calculated from 10^6 independent runs of up to 10^5 time steps at each r value.

The analysis presented in Fig. 3 gives a critical repulsion value of $r_c = 0.7435(15)$. We find values of $\delta = 0.287(4)$, $\eta = 0.003(4)$, $\eta_o = 0.306(5)$, and $z = 1.146(8)$ for the critical exponents. From these values we determine the bicritical behavior falls in the BAWe universality class, for which [14] the exponents are $\delta = 0.285(2)$, $\eta = 0.000(1)$, and $z = 1.141(2)$. The value of η_o does not agree very well with the scaling law $\eta_o = (z/2) - \delta$ derived above, but that is the result of the effect of the second term in Eq. (8), which acts as a large correction to the asymptotic time behavior. The agreement with the scaling law improves when the data for n_o is fit using the form (8) with the exponents z, δ and η fixed and the coefficients c_1 and c_2 are fitted.

Figure 4 shows the results from the interface dynamics simulations, for three values of r near $r_c = 0.7435(15)$. From 10^7 independent runs of up to 10^5 time steps we find values of $\delta' = 0.700(10)$, $\eta' = -0.404(9)$, and $z' = 1.153(6)$. This type of simulation gives us information about the competition between the growth of the two saturated phases that is not gained in the defect dynamics type of simulations. First, notice that z', the exponent governing the size of the interface, equals z. Also, although δ' and η' have different values than their defect dynamics cousins, the sum $(\delta' + \eta')$, which controls the time evolution of the number of vacancies in just the surviving runs, is the same as $(\delta + \eta)$ within statistical error. This indicates that the critical spreading of the defect is insensitive as to whether it is bordered on each side by the same saturated phase or by two different, though equivalent, saturated phases. The independent dynamical exponent δ' measured here agrees with the value found in the three-species model [12,13], suggesting that its value is universal.

V. SUMMARY

We have investigated the behavior of an interacting one-dimensional adsorption-limited monomer-monomer model. The like-neighbor repulsion in the model leads to the presence of a large reactive region and a bicritical point – inaccurately termed a tricritical point in Ref. [17] – where the first-order discontinuous transition between the two symmetric saturated phases meets the two continuous transitions from either saturated phase to the reactive phase. We have used two types of epidemic simulations to study the behavior of the system at the bicritical point. Using the defect dynamics simulations we determine the bicritical behavior falls in the BAWe universality class. With the interface dynamics we measure a new universal number δ', related to the probability that a minimum-width interface between the two saturated phases will avoid collapse back to its minimum size. It

would be interesting to measure the exponent δ' for other models in which two symmetric adsorbing phases meet a reactive phase. In addition, by comparing the results from the two types of simulations we find that the time evolution of the number of vacancies in the lattice in the surviving runs is the same in both cases. This suggests that the critical spreading of a localized defect is insensitive to initial conditions, and the characteristic fluctuations in the domain walls behave differently than a defect in a homogeneous phase.

The failure of mean field theory to describe the qualitative features of the phase diagram, even when clusters of triples of sites were included, points to the importance of large domains of each species in the vicinity of the bicritical point. The large domains, which are clearly apparent in static Monte Carlo simulations, are the necessary background for the simplest dynamical variables needed to describe the bicritical point, namely, the domain walls. The random walks of these walls, coupled with the fact that their number is conserved modulo 2, are the crucial ingredients in the critical behavior at the bicritical point.

This work was supported by the National Science Foundation under Grant No. DMR–9408634.

REFERENCES

[1] H. K. Janssen, Z. Phys. B **42**, 151 (1981).
[2] P. Grassberger, Z. Phys. B **47**, 365 (1982).
[3] T. E. Harris, Ann. Prob. **2**, 969 (1974).
[4] T. Aukrust, D. A. Browne, and I. Webman, Phys. Rev. A **41**, 5294 (1990).
[5] H. Takayasu and A. Yu. Tretyakov, Phys. Rev. Lett. **68**, 3060 (1992).
[6] I. Jensen, Phys. Rev. E **47**, 1 (1993); J. Phys. A **26**, 3921 (1993).
[7] J. L. Cardy and R. L. Sugar, J. Phys. A **13**, L423 (1980).
[8] G. Grinstein, Z.-W. Lai, and D. A. Browne, Phys. Rev. A **40**, 4820 (1989); I. Jensen, H. C. Fogedby, and R. Dickman, *ibid.* **41**, 3411 (1990).
[9] P. Grassberger, F. Krause, and T. von der Twer, J. Phys. A **17**, L105 (1984); P. Grassberger, J. Phys. A **22**, L1103 (1989).
[10] N. Menyhárd, J. Phys. A **27**, 6139 (1994); N. Menyhárd and G. Ódor, J. Phys. A **28**, 4505 (1995); N. Menyhárd and G. Ódor, preprint (1996).
[11] M. H. Kim, and H. Park, Phys. Rev. Lett. **73**, 2579 (1994); H. Park, and H. Park, Physica A **221**, 97 (1995); H. Park, M. H. Kim, and H. Park, Phys. Rev. E **52**, 5664 (1995).
[12] K. E. Bassler and D. A. Browne, Phys. Rev. Lett. **77**, 4094 (1996).
[13] K. E. Bassler and D. A. Browne, to be published in May 1 issue of Physical Review E.
[14] I. Jensen, Phys. Rev. E **50**, 3623 (1994).
[15] J. Cardy and U. Taüber, has appeared in Phys. Rev. Lett. (1996).
[16] M. E. Fisher and D. R. Nelson, Phys. Rev. Lett. **32**, 1350 (1974).
[17] J. Zhuo, S. Redner, and H. Park, J. Phys. A: Math. Gen. **26**, 4197 (1993).
[18] E. Wicke, P. Kumman, W. Keil, and J. Scheifler, Ber. Bunsenges. Phys. Chem. **4**, 315 (1980); R. M. Ziff and K. A. Fitchthorn, Phys. Rev. B **34**, 2038 (1986); K. A. Fitchthorn, E. Gulari, and R. M. Ziff, in: *Catalysis 1987*, ed. J. W. Ward, (Elsevier, 1987); D. ben-Avraham, D. B. Considine, P. Meakin, S. Redner, and H. Takayasu, J. Phys. A **23**, 4297 (1990); D. B. Considine, H. Takayasu, and S. Redner, J. Phys. A **23**, L1181 (1990); J. W. Evans and M. S. Miesch, Phys. Rev. Lett. **66**, 833 (1991).
[19] E. Clément, P. Leroux-Hugon, and L. M. Sander, Phys. Rev. Lett. **67**, 1661 (1991); P. L. Krapivsky, Phys. Rev. A **44**, 1067 (1992); J. Phys. A **25**, 5831 (1992); J. W. Evans and T. R. Ray, Phys. Rev. E **47**, 1018 (1993); D. S. Sholl and R. T. Skodje, Phys. Rev. E **53**, 335 (1996).
[20] R. Dickman, Phys. Rev. A **34**, 4626 (1986).
[21] P. Grassberger, J. Phys. A **22**, 3673 (1989); P. Grassberger and A. de la Torre, Ann. Phys. (New York) **122**, 373 (1979).
[22] P. Grassberger, J. Phys. A **22**, 3673 (1989); P. Grassberger and A. de la Torre, Ann. Phys. (New York) **122**, 373 (1979).

TABLES

A adsorption	Rate	B adsorption	Rate
$VVV \rightarrow VAV$	p	$VVV \rightarrow VBV$	q
$VVA \rightarrow VAA$	$p\,r$	$VVA \rightarrow VVV$	$q\,r$
$AVV \rightarrow AAV$	$p\,r$	$AVV \rightarrow VVV$	$q\,r$
$AVA \rightarrow AAA$	$p\,r$	$AVA \rightarrow AVV$	$\frac{1}{2}q\,r$
		$AVA \rightarrow VVA$	$\frac{1}{2}q\,r$
$VVB \rightarrow VVV$	p	$VVB \rightarrow VBB$	$q\,r$
$BVV \rightarrow VVV$	p	$BVV \rightarrow BBV$	$q\,r$
$BVB \rightarrow BVV$	$\frac{1}{2}p\,r$	$BVB \rightarrow BBB$	$q\,r$
$BVB \rightarrow VVB$	$\frac{1}{2}p\,r$		
$AVB \rightarrow AVV$	$p\,r$	$AVB \rightarrow VVB$	$q\,r$
$BVA \rightarrow VVA$	$p\,r$	$BVA \rightarrow BVV$	$q\,r$

TABLE I. Rates for all allowed kinetic processes. The adsorption is attempted on the middle site in each case

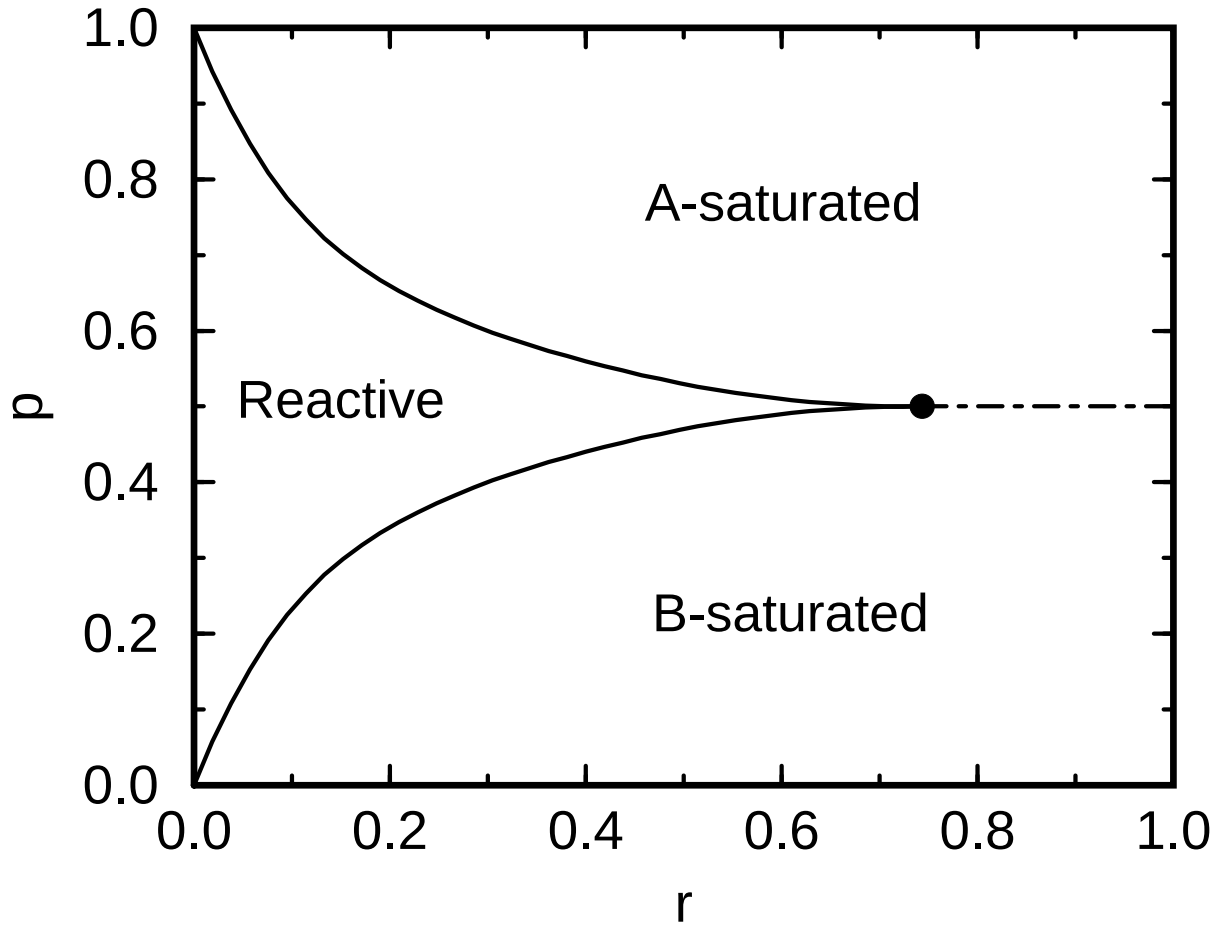

FIG. 1. Phase diagram determined by Monte Carlo simulation for the interacting monomer-monomer model. The continuous transitions from either of the saturated phases (A and B) to the reactive phase are shown as solid lines, while the transition between the two saturated phases (dot-dash line) is first-order. The three phases coexist at a bicritical point at $(r_c, p_c) = (0.7435, 0.5)$, which is shown as a heavy dot.

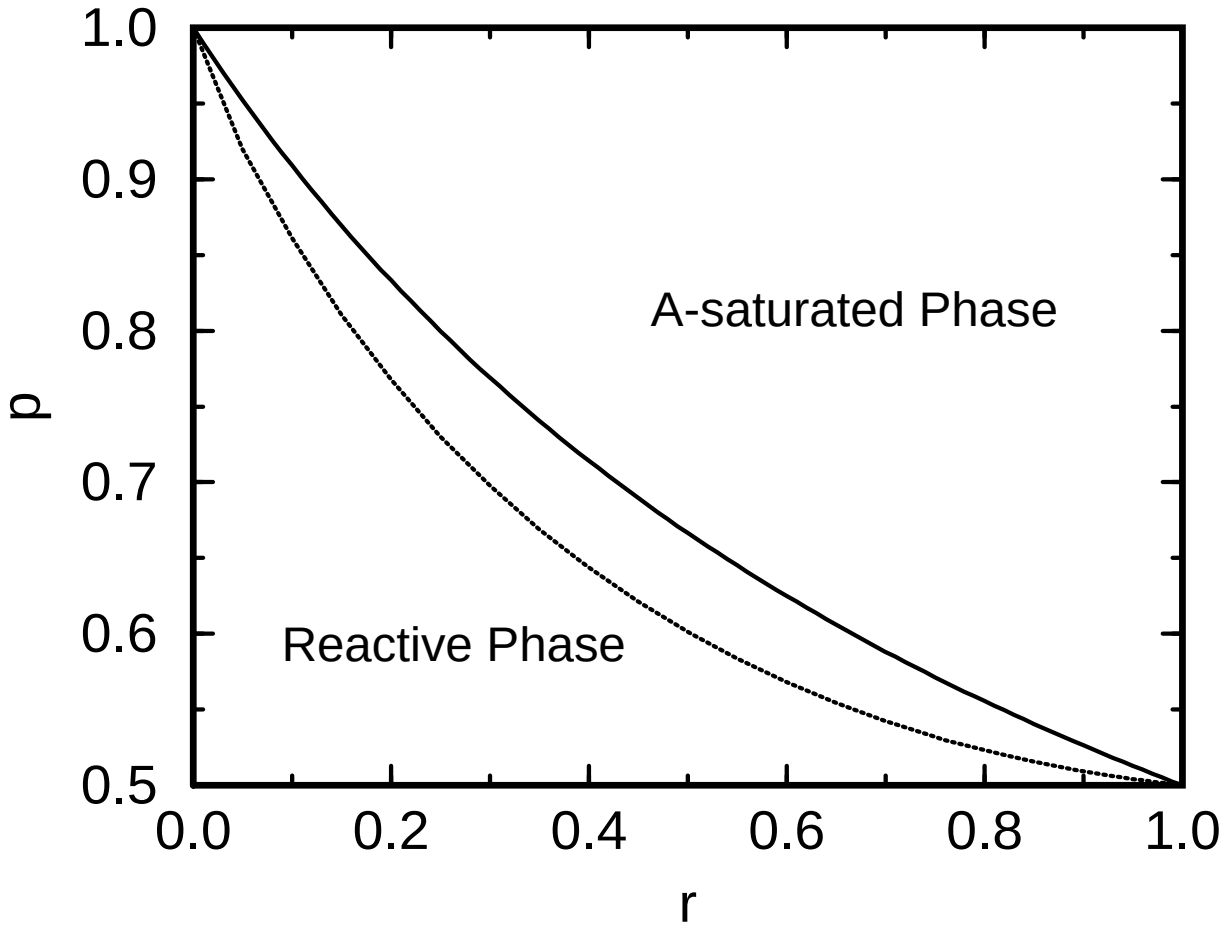

FIG. 2. Phase boundary between the A-saturated and reactive phases in the site approximation (solid line) and pair approximation (dashed line). The triple approximation is indistinguishable from the pair approximation on this figure.

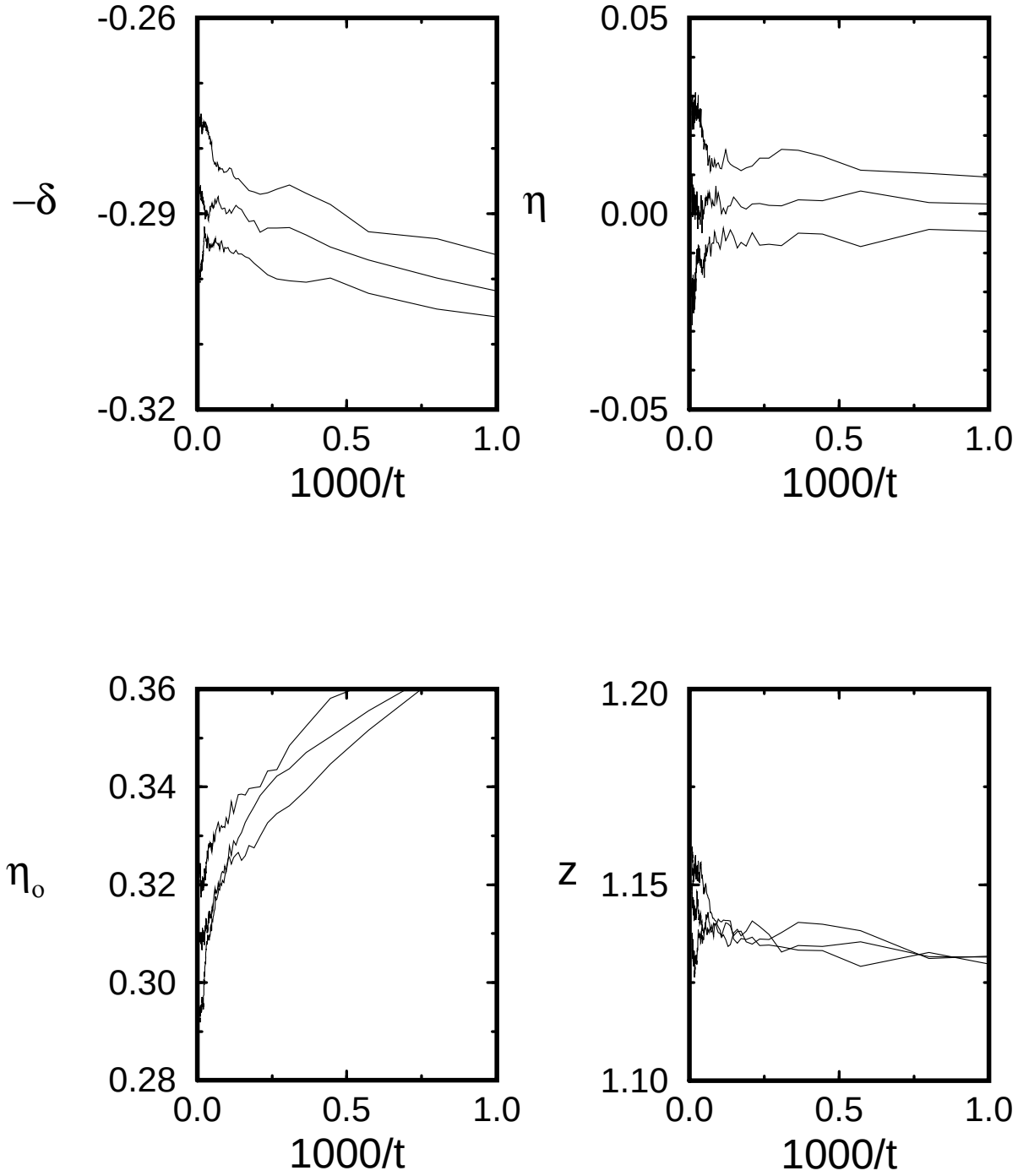

FIG. 3. Effective exponents for the bicritical defect dynamics. The three curves correspond to three values of r near the bicritical point. From top to bottom they are $r = 0.7420, 0.7435, 0.7450$, with the middle curves corresponding to the bicritical values.

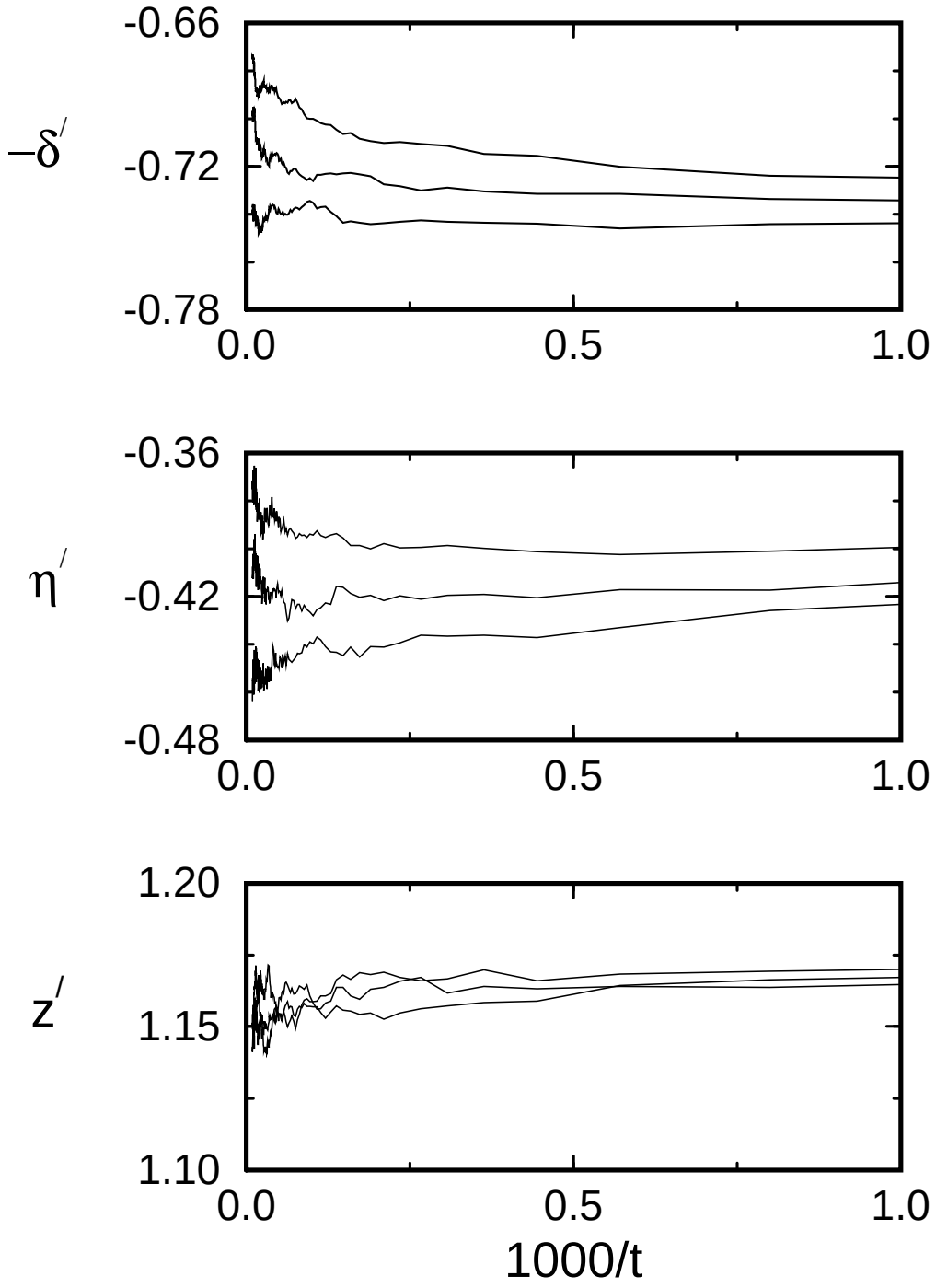

FIG. 4. Effective exponents for the bicritical interface dynamics. The three curves correspond to three values of r near the bicritical point. From top to bottom they are $r = 0.7420, 0.7435, 0.7450$, with the middle curve corresponding to the bicritical value.